23rd International Congress on Sound & Vibration
Athens, Greece 10-14 July 2016
ICSV23

ANALYSIS OF FLAME-INTRINSIC INSTABILITY IN A RESONATOR

Nalini Mukherjee, Maria Heckl and Victor Shrira

Faculty of Natural Sciences, Keele University, Staffordshire ST5 5BG, UK

This study is aimed at understanding the recently discovered phenomenon of flame-intrinsic modes inside an acoustic resonator in the context of thermoacoustic instabilities in a combustion chamber. Earlier studies have shown the existence of intrinsic thermoacoustic modes, which are qualitatively different from the well-known acoustic modes. The analytical results were limited to intrinsic modes in an infinite system. Here we examine properties of intrinsic thermoacoustic modes within the framework of a one-dimensional resonator containing a heat source modelled by the linear $n\tau$-law. In the limit of small values of the interaction index n, we find an explicit dispersion relation for the intrinsic modes: there is always infinite number of these modes and for small n these modes are heavily damped. To leading order, the frequencies of these modes depend neither on the properties of the resonator nor on the position of the flame. Numerical analysis of the system for larger values of n shows that with the increase of n the real part of the frequency for each intrinsic mode changes very slightly and this small frequency shift depends both on the properties of the resonator and position of the flame; the decay rate sharply decreases with n and for sufficiently large n, the mode becomes unstable.

1. Introduction

The development of low-emission combustion systems is a high priority for environmental reasons. This is achieved with a technology that is based on lean premixed combustion. However, such combustion systems are particularly susceptible to thermoacoustic instabilities, i.e. high-amplitude pressure oscillations that may cause serious hardware damage. This phenomenon has received a lot of attention from researchers worldwide (see e.g. [1]). Until recently, the conventional wisdom was that thermoacoustic instabilities are caused by a complex interplay between various physical processes, the two key ones being:

(1) A flame with an unsteady heat release rate acts like an acoustic monopole source, generating acoustic waves (driving process)
(2) Acoustic waves in a combustion chamber are reflected at its boundaries, return to the flame and perturb its heat release rate (feedback process).

The feedback between these processes may lead to an oscillation with growing amplitude and with a frequency that is typically close to one of the eigenfrequencies of the combustion chamber.

However, very recent studies have shown that there is an alternative feedback loop leading to the generation of the so-called *intrinsic thermoacoustic* (ITA) instabilities, which can occur even if the feedback process mentioned above is missing.

Hoeijmakers et al [2] demonstrated experimentally that ITA modes do exist. In a subsequent analytical study [3], they derived the dispersion relation for the frequencies of the intrinsic modes in an idealised setup with the following features: 1-D tube with non-reflecting ends, flame described by the $n\tau$-model, piecewise constant temperature distribution in the tube with a jump at the flame from $\overline{T}_1$ (cold) to $\overline{T}_2$ (hot). They solved the dispersion relation and found the complex frequency values

$$\omega_m = \frac{1}{\tau}(1+2m)\pi - \mathrm{i}\frac{1}{\tau}\ln\frac{\varepsilon+1}{n\theta}, \quad \text{with } m = 0, \pm 1, \pm 2, \ldots \tag{1}$$

where i is the imaginary unit, $\theta = \overline{T}_2/\overline{T}_1 - 1$ is the temperature jump, and $\varepsilon = (\overline{\rho}_1 c_1)/(\overline{\rho}_2 c_2)$ is the jump in specific acoustic impedance across the flame. The integer m is the mode number.

Bomberg et al [4] gave a physical explanation how ITA modes are generated. The underlying mechanism is again a feedback loop: A velocity disturbance travelling upstream towards the flame modulates the heat release rate, which in turn generates an acoustic wave; the upstream-travelling part of this wave influences the velocity and thus closes the feedback loop. In a companion study by Emmert et al [5], the stability of intrinsic modes is investigated from the viewpoint of a balance of the acoustic energy across the flame.

Detailed numerical studies (Courtine et al [6], Silva et al [7]), where a flame placed in an acoustically anechoic environment is modelled by direct numerical simulation (DNS), have since then shown that the ITA feedback proposed in [4] is a genuine physical phenomenon, and not just a spurious by-product of simplistic network models.

The aim of our paper is to investigate ITA modes of a flame situated in an *acoustic resonator*, rather than in an anechoic environment as in previous studies. Our approach is largely analytical.

2. Mathematical model

We consider the idealised combustion system sketched in figure 1. Effectively, this is a quarter-wave resonator with a closed end at $x = 0$ and an open end at $x = L$. There is a dump plane at $x = x_q$, where the cross-sectional area jumps from S_1 to S_2. The flame is compact and situated at x_q. Also at x_q, there is a jump in mean temperature from $\overline{T}_1$ (cold) to $\overline{T}_2$ (hot), and a corresponding jump in mean density from $\overline{\rho}_1$ to $\overline{\rho}_2$, and in speed of sound from c_1 to c_2.

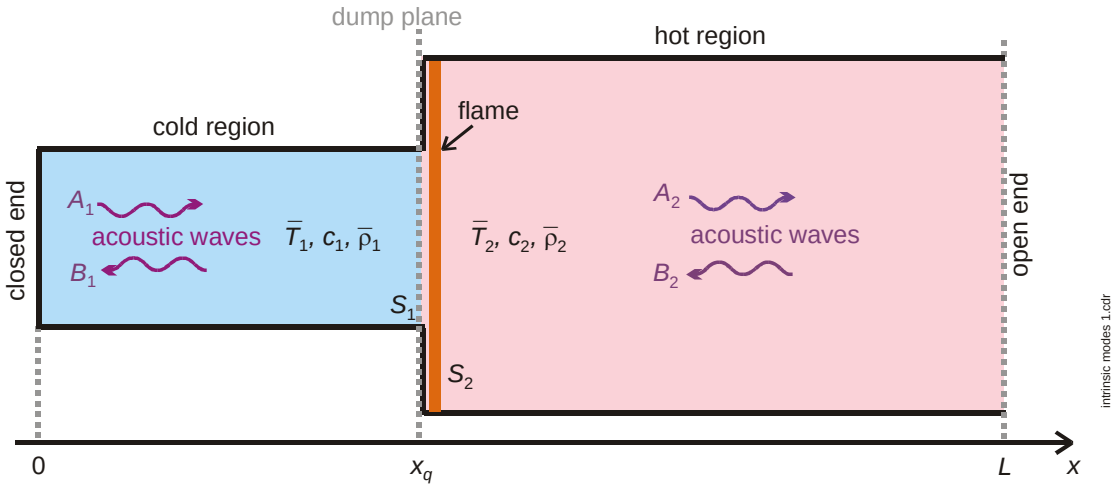

Figure 1: Schematic of the combustion system under consideration.

The acoustic pressure and velocity are denoted by p' and u' respectively, and can be written as

$$p_1'(x) = A_1 \mathrm{e}^{\mathrm{i}k_1 x} + B_1 \mathrm{e}^{-\mathrm{i}k_1 x}, \quad u_1'(x) = \frac{1}{\overline{\rho}_1 c_1}\left[A_1 \mathrm{e}^{\mathrm{i}k_1 x} - B_1 \mathrm{e}^{-\mathrm{i}k_1 x}\right], \tag{2a,b}$$

$$p_2'(x) = A_2 \mathrm{e}^{\mathrm{i}k_2 x} + B_2 \mathrm{e}^{-\mathrm{i}k_2 x}, \quad u_2'(x) = \frac{1}{\overline{\rho}_2 c_2}\left[A_2 \mathrm{e}^{\mathrm{i}k_2 x} - B_2 \mathrm{e}^{-\mathrm{i}k_2 x}\right], \tag{3a,b}$$

where the time dependence $\mathrm{e}^{-\mathrm{i}\omega t}$ has been omitted. $k_1 = \omega/c_1$ and $k_2 = \omega/c_2$ are wave numbers. A_1 and A_2 are pressure amplitudes of downstream-travelling waves, and B_1 and B_2 of upstream-travelling waves. They are related by the following boundary conditions:

$$\frac{A_1}{B_1} = 1 \text{ (closed end at } x = 0\text{)}, \qquad \frac{B_2 \mathrm{e}^{-\mathrm{i}k_2 L}}{A_2 \mathrm{e}^{\mathrm{i}k_2 L}} = -1 \text{ (open end at } x = L\text{)}. \tag{4a,b}$$

A compact flame with unsteady rate of heat release Q' acts like a monopole-type sound source [8]: the pressure across it is continuous (momentum conservation),

$$p_1'(x_q) = p_2'(x_q), \tag{5}$$

and the volume flow across the flame jumps by $(\gamma - 1)/c_1^2\, Q'$, i.e. by the volume outflow from the source region (mass conservation),

$$S_1 \bar{\rho}_1 u_1'(x_q) - S_2 \bar{\rho}_2 u_2'(x_q) = -\frac{\gamma - 1}{c_1^2} Q'; \tag{6}$$

γ is the specific heat ratio.

We model the flame by a simple linear time-lag law [9],

$$Q'(t) = \frac{\bar{\rho}_1 S_1 c_1}{\gamma - 1}\, n\, u'(x_q, t - \tau), \tag{7}$$

where n is the interaction index, and τ is the time-lag. In the frequency domain, this has the form

$$\hat{Q}(\omega) = \frac{\bar{\rho}_1 S_1 c_1}{\gamma - 1}\, n\, \mathrm{e}^{\mathrm{i}\omega\tau}\, \hat{u}'(x_q, \omega). \tag{8}$$

The two conservation eqs. (5) and (6) can be written in terms of the pressure amplitudes A_1, A_2, B_1, B_2 by substituting with eqs. (2) and (3). Together with (4a,b), this yields 4 homogeneous equations for the 4 amplitudes:

$$\begin{bmatrix} 1 & -1 & 0 & 0 \\ \mathrm{e}^{\mathrm{i}k_1 x_q} & \mathrm{e}^{-\mathrm{i}k_1 x_q} & -\mathrm{e}^{\mathrm{i}k_2 x_q} & -\mathrm{e}^{-\mathrm{i}k_2 x_q} \\ (1 + n\mathrm{e}^{\mathrm{i}\omega\tau})\mathrm{e}^{\mathrm{i}k_1 x_q} & (-1 - n\mathrm{e}^{\mathrm{i}\omega\tau})\mathrm{e}^{-\mathrm{i}k_1 x_q} & -(S_2/S_1)(c_1/c_2)\mathrm{e}^{\mathrm{i}k_2 x_q} & (S_2/S_1)(c_1/c_2)\mathrm{e}^{-\mathrm{i}k_2 x_q} \\ 0 & 0 & \mathrm{e}^{\mathrm{i}k_2 L} & \mathrm{e}^{-\mathrm{i}k_2 L} \end{bmatrix} \begin{bmatrix} A_1 \\ B_1 \\ A_2 \\ B_2 \end{bmatrix} = \begin{bmatrix} 0 \\ 0 \\ 0 \\ 0 \end{bmatrix} \tag{9}$$

The determinant of the 4×4 matrix has to be zero, and this generates the dispersion relation

$$\begin{aligned} f(\omega) = {} & [(S_2/S_1)(c_1/c_2) + 1]\cos[k_2(L - x_q) + k_1 x_q] + \\ & + [(S_2/S_1)(c_1/c_2) - 1]\cos[k_2(L - x_q) - k_1 x_q] - 2n\mathrm{e}^{\mathrm{i}\omega\tau} \sin k_1 x_q \sin[k_2(L - x_q)] = 0; \end{aligned} \tag{10}$$

we call $f(\omega)$ the characteristic function.

For the special case, where the cross-section and mean temperature are uniform ($S_1 = S_2$, $\bar{T}_1 = \bar{T}_2$), the wave numbers are identical, $k_1 = k_2 = k$, and the dispersion relation (10) reduces to

$$\cos kL - n\mathrm{e}^{\mathrm{i}\omega\tau} \sin kx_q \sin[k(L - x_q)] = 0. \tag{11}$$

For a flame located exactly halfway along the tube ($x_q = L/2$), this reduces further to

$$\cos kL = \frac{n\mathrm{e}^{\mathrm{i}\omega\tau}}{2 + \mathrm{e}^{\mathrm{i}\omega\tau}}\ . \tag{12}$$

The solution of the dispersion relation gives the frequencies ω of all modes. These frequencies are generally complex; the real part gives the oscillation frequency of the mode, and the imaginary part gives the growth rate.

3. Analytical expression for the intrinsic modes

We now try to find the roots of the dispersion relation analytically by turning to eq. (12). For very small values of n, this equation has two sets of roots:

(1) the conventional acoustic modes, described by $\cos kL = 0$,

(2) a new set of modes, for which $e^{i\omega\tau}$ is very large, i.e. the imaginary part of ω is highly negative; this represents strongly damped modes. We explain this with a simple order-of-magnitude analysis: For a damped mode, the modulus of the denominator in (12) exceeds 2, hence for nonzero $\cos kL$, there is only one possibility for (12) to have solutions: the numerator $ne^{i\omega\tau}$ has to be $O(1)$. This implies that when n is small, $e^{i\omega\tau}$ has to be large.

In order to examine these new modes further, we express the functions cos and sin in eq. (10) by using Euler's formula,

$$\cos\alpha = (e^{i\alpha} + e^{-i\alpha})/2, \qquad \sin\alpha = (e^{i\alpha} - e^{-i\alpha})/(2i). \tag{13a,b}$$

This leads to

$$\begin{aligned}&[(S_2/S_1)(c_1/c_2)+1](e^{i[k_2(L-x_q)+k_1x_q]} + e^{-i[k_2(L-x_q)+k_1x_q]})\\ &+[(S_2/S_1)(c_1/c_2)-1](e^{i[k_2(L-x_q)-k_1x_q]} + e^{-i[k_2(L-x_q)-k_1x_q]})\\ &+ne^{i\omega\tau}(e^{ik_1x_q} - e^{-ik_1x_q})(e^{ik_2(L-x_q)} - e^{-ik_2(L-x_q)}) = 0.\end{aligned} \tag{14}$$

We then divide both sides of this equation by the expression $e^{i[(k_2-k_1)x_q+k_2L]}$ and obtain

$$\begin{aligned}&[(S_2/S_1)(c_1/c_2)+1](1+e^{-2i[(k_2(L-x_q)+k_1x_q]}+1)+\\ &+[(S_2/S_1)(c_1/c_2)-1](e^{-2ik_1x_q} + e^{-2ik_2(L-x_q)})\\ &+ne^{i\omega\tau}(1-e^{-2ik_2(L-x_q)} - e^{-2ik_1x_q} + e^{-2i[k_2(L-x_q)+k_1x_q]}) = 0.\end{aligned} \tag{15}$$

For the new set of modes, the imaginary part of ω, and hence also of the wave numbers k_1, k_2 is highly negative. The exponential expressions containing k_1 or k_2 in (15) are therefore much smaller than 1, and can be neglected. This leaves

$$[(S_2/S_1)(c_1/c_2)+1] + ne^{i\omega\tau} = 0. \tag{16}$$

This has explicit analytical solutions,

$$\omega_m = \frac{1}{\tau}(2m+1)\pi - i\frac{1}{\tau}\ln\frac{(S_2/S_1)(c_1/c_2)+1}{n}, \tag{17}$$

where $m = 0, \pm1, \pm2, \ldots$ is an integer, which represents the mode number. This expression is identical with equation (1), which gives the expression found by [3] for an $n\tau$-flame in an *infinitely long* tube. The real part of the frequencies depends linearly on the mode number, it depends inversely on the time-lag τ, but it is independent on the interaction index n (in the adopted limit of small n). The imaginary part is the same for all mode numbers, and it depends inversely on the time-lag and logarithmically on the interaction index. The complex frequencies given by (17) do not depend on the flame position, nor on the tube length.

4. Numerical analysis for the intrinsic and acoustic modes

In this section, we determine the complex eigenfrequencies for both types of modes (acoustic and intrinsic) by considering the full dispersion relation (10), and solving it numerically. The combustion system has the following properties: $L = 0.75$m (total tube length), $x_q = L/2$ (flame position), $\bar{T}_1 = \bar{T}_2 = 297$K (room temperature throughout), $c_1 = c_2 = 345$m/s (speed of sound), and

$\bar{\rho}_1 = \bar{\rho}_2 = 1.2\text{kg/m}^3$ (mean density). These represent the properties of the laminar V-flame test rig at IIT Madras [10].

4.1 Dependence of the modal frequencies on time-lag and interaction index

Figure 2 shows the dependence of the modal frequencies (real part) on the time-lag for the range $\tau = 1 \ldots 5\,\text{ms}$ for three specific n-values ($n = 0,\ 0.25,\ 1$); figure 3 shows the dependence on the interaction index for the range $n = 0, \ldots 1.5$ for the specific time-lag $\tau = 5\text{ms}$, and for two tube lengths ($L = 0.75\text{m}$ and $L = 0.38\text{m}$). The frequency range shown in both figures is $0 \ldots 1000\text{Hz}$. The acoustic modes are marked by blue squares, and the intrinsic modes by red/pink circles. Also shown (red curve) is the analytical solution for the intrinsic modes given by the real part of eq. (17).

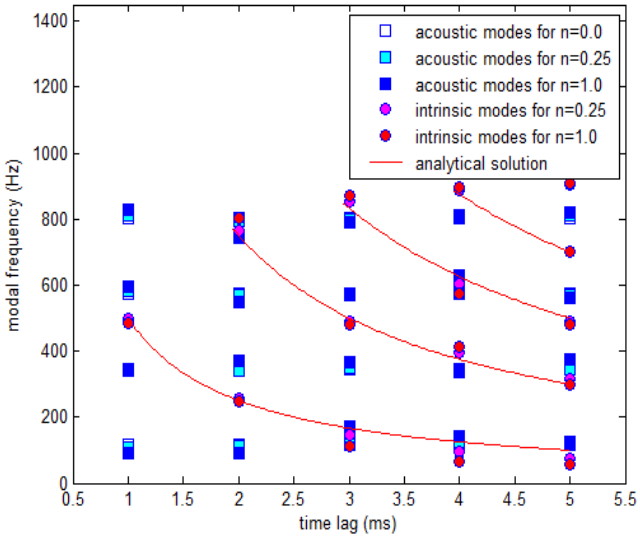

Figure 2: Modal frequencies vs. τ ($n = 0,\ 0.25,\ 1$).

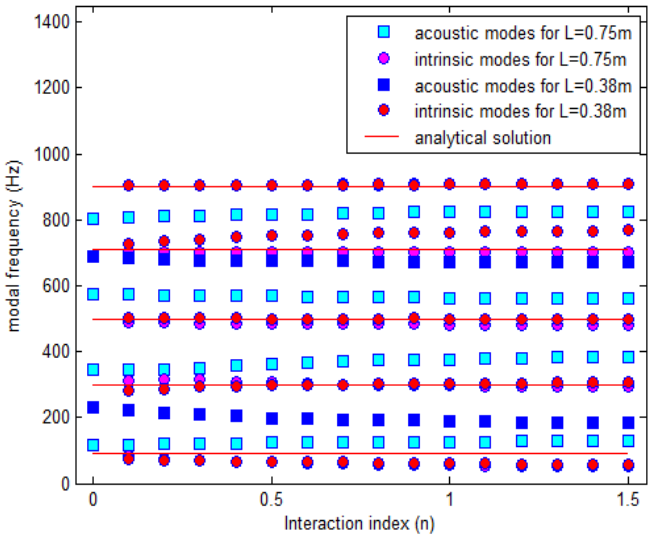

Figure 3: Modal frequencies vs. n ($\tau = 5\,\text{ms}$).

As expected, the acoustic modes have frequencies close to those of a quarter-wave resonator, ($f_0,\ 3f_0,\ 5f_0, \ldots$, where f_0 is the fundamental frequency), and they are not affected much by changes in τ or n. The intrinsic modes show a strong dependence on the time-lag (see figure 2): their frequencies decay with increasing time-lag. The decay closely follows the analytical curve, which is a $1/\tau$ hyperbola. The dependence of the modal frequency on the interaction index is weak for all modes (see figure 3). Again, the analytical (red) curve is a good approximation for the numerical results. Figure 3 also shows the effect of changing the tube length. The acoustic modes show a strong response to this (halving the tube length doubles their frequencies), but the intrinsic modes are barely affected (in most cases the pink and red circles coincide and cannot be distinguished).

4.2 Stability behaviour of the intrinsic and acoustic modes

In this section, we illustrate the behaviour of the acoustic and intrinsic modes by contour plots in the complex frequency plane. Curves depicting constant values of $|f(\omega)|$, where $f(\omega)$ is given by eq. (10) will be shown. The modal frequencies are situated at points where $|f(\omega)| = 0$. These are surrounded by closed loops, where $|f(\omega)|$ has values close to zero.

Figure 4 shows such a plot for a small n value and medium time-lag: $n = 0.025$, $\tau = 3\text{ms}$. For reasons of scale, this plot has been split into two sections. The acoustic modes (marked by little blue squares) all have growth rates around 0 and are shown in the top-section of the plot. The intrinsic modes (marked by little green squares) have highly negative growth rates, between $-1400\,\text{s}^{-1}$ and $-1500\,\text{s}^{-1}$, and they are shown in the bottom section.

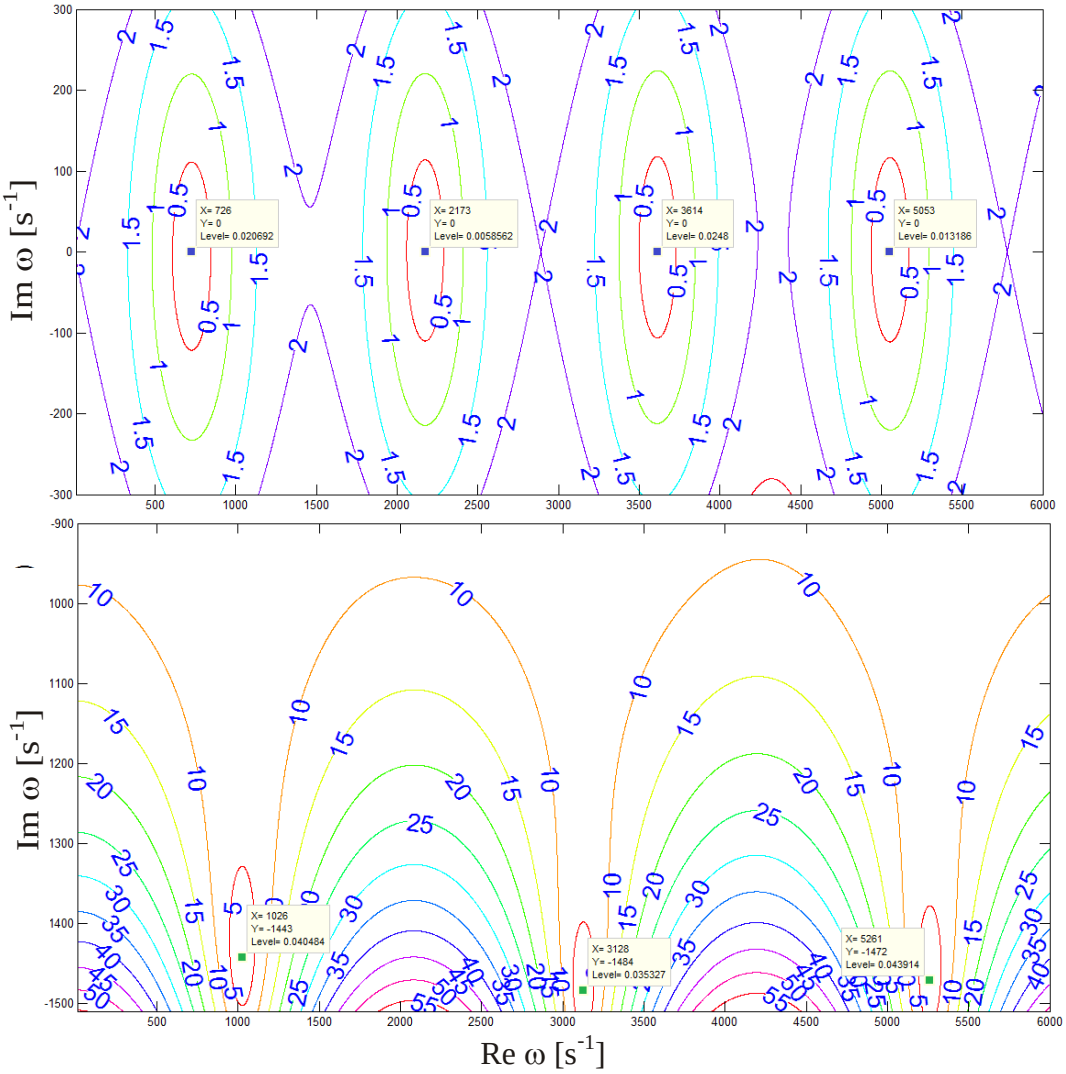

Figure 4: Contour plot of $|f(\omega)|$ in the complex frequency plane for $n = 0.025$, $\tau = 3\,\text{ms}$. The two sections are parts of the same contour plot.

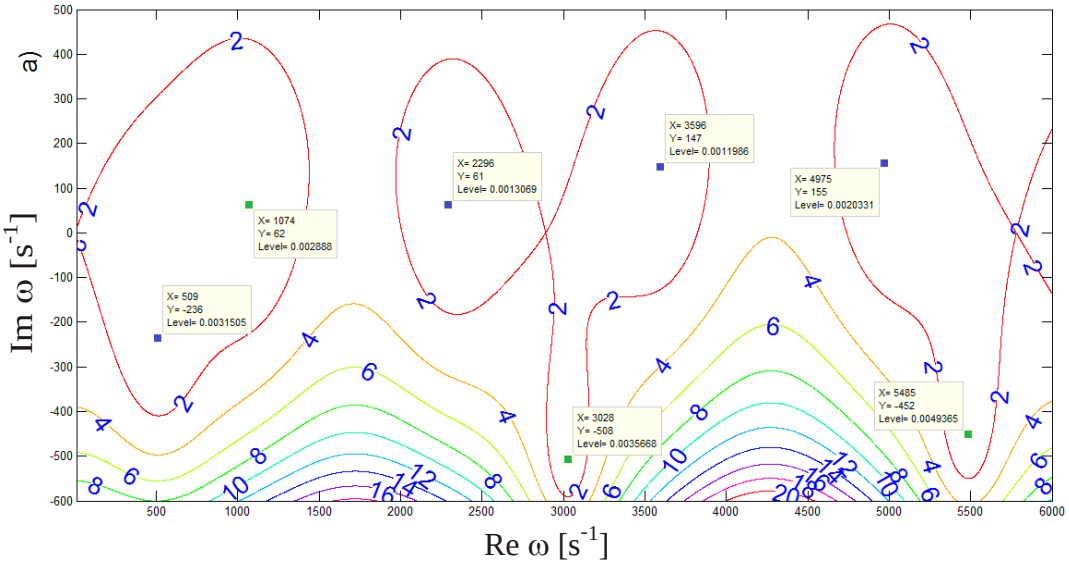

Figure 5: Contour plot of $|f(\omega)|$ in the complex frequency plane for $n = 1$, $\tau = 3\,\text{ms}$.

We illustrate the effect of increasing the interaction index n by figure 5, which shows the contour plot of $|f(\omega)|$ for $n = 1$, $\tau = 3\text{ms}$. The increase in n has a strong effect on the intrinsic modes

in that their growth rate increases dramatically. The lowest intrinsic mode (which has a frequency of around $1000s^{-1}$) has even changed the sign of its growth rate and become unstable. Further numerical studies (not shown here) show that there is a threshold value on n above which mode any mode becomes unstable.

Figure 6 shows the effect of increasing the time-lag to $\tau = 5$ ms, leaving the interaction index as in the previous figure. The intrinsic modes undergo a drop in the modal frequency.

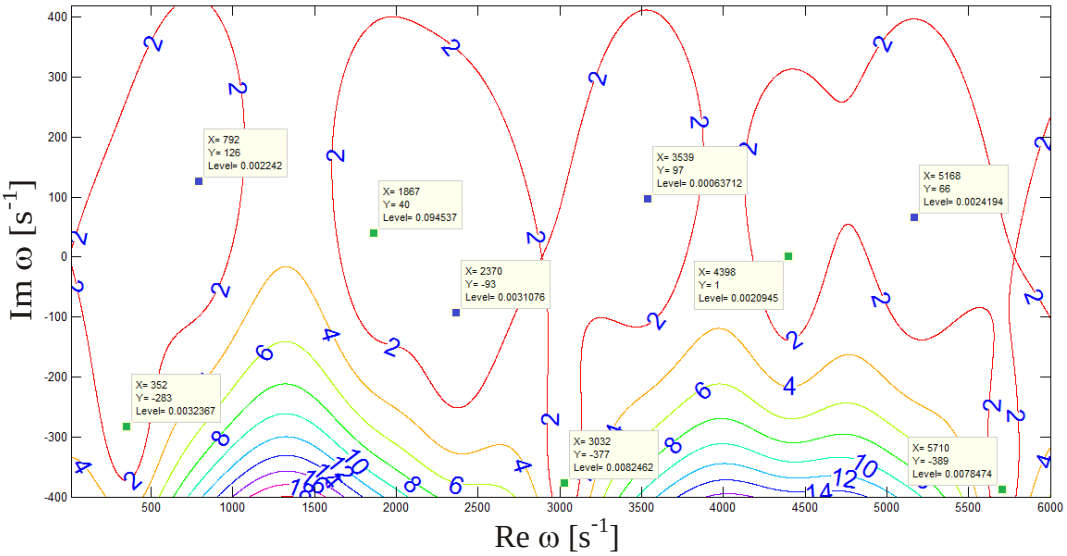

Figure 6: Contour plot of $|f(\omega)|$ in the complex frequency plane for $n = 1$, $\tau = 5$ ms.

4.3 Effect of area expansion and temperature jump

The effect of other parameters, such as the area expansion S_2 / S_1 or the temperature jump across the flame, can be investigated in the same way. We do this here for the area expansion. Figure 7 shows the case $S_2 / S_1 = 1.5$; the parameters n and τ are the same as in figure 6 to allow comparison. We observe that the intrinsic modes have become more stable; this is in line with [6], where the same effect is observed with DNS.

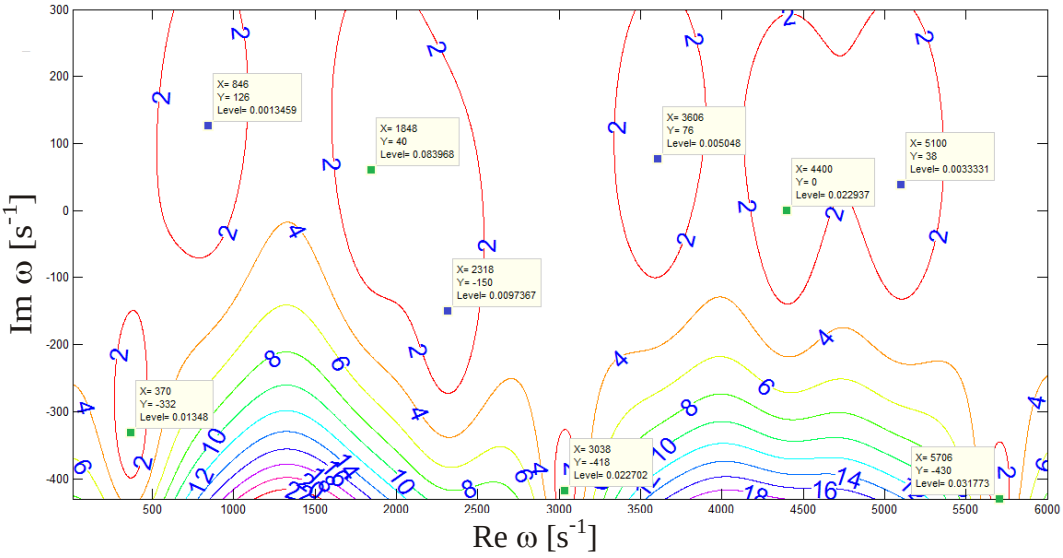

Figure 7: Contour plot of $|f(\omega)|$ for area expansion $S_2 / S_1 = 1.5$ ($n = 1$, $\tau = 5$ ms).

We have also investigated the effect of a jump in mean temperature by increasing $\bar{T}_2$, while leaving $\bar{T}_1$ at room temperature. Our results (not shown here) indicate that the jump has a destabilising effect on the intrinsic modes.

5. Conclusions

We summarise our main advance in understanding intrinsic thermoacoustic modes in resonators as follows:

(i) For any nonzero n and τ there is always an infinite set of intrinsic modes.

(ii) For small n, we derived an explicit dispersion relation (16) for the intrinsic modes to leading order; this dispersion relation is identical with that found for an anechoic situation. The solutions of this dispersion relation, i.e. the complex eigenfrequencies of the intrinsic modes, have a highly negative imaginary part, and a real part given by $(2m+1)\pi/\tau$, i.e. these are strongly damped, and their modal frequency depends strongly on the time-lag.

(iii) By solving the dispersion relation numerically, we showed that an increase in n has little effect on the modal frequencies (the frequency shift does not exceed 5%), but it leads to a strong increase of the growth rate.

(iv) The small frequency shift and the threshold value of n do depend on characteristics of the resonator and on the flame position; at present we find them by solving the eigenvalue problem numerically.

Our analysis is limited to situations where the intrinsic and acoustic modes are well-separated.

Acknowledgement

The presented work is part of the Marie Curie Initial Training Network "Thermoacoustic and Aeroacoustic Nonlinearities in Green combustors with Orifice structures" (TANGO). We gratefully acknowledge the financial support from the European Commission under call FP7-PEOPLE-ITN-2012.

REFERENCES

1 Lieuwen, T.C. and Yang, V. *Combustion instabilities in gas turbine engines*. American Institute of Aeronautics and Astronautics, (2005).

2 Hoeijmakers, P.G.M., Lopez, I., Kornilov, V., Nijmeijer, H. and de Goey, L P H. Experimental investigation of intrinsic flame stability. *Proceedings of the European Combustion Meeting, Lund, Sweden, 25 – 28 June 2013.*

3 Hoeijmakers, M., Kornilov, V., Arteaga, I.L., de Goey, P. and Nijmeijer, H. Intrinsic instability of flame-acoustic coupling. *Combustion and Flame* **161**, 2860-2867, (2014).

4 Bomberg, S., Emmert, T. and Polifke, W. Thermal versus acoustic response of velocity sensitive premixed flames. *Proceedings of the Combustion Institute* **35**, 3185-3192, (2015).

5 Emmert, T., Bomberg, S. and Polifke, W. Intrinsic thermoacoustic instability of premixed flames. *Combustion and Flame* **162**, 75-85, (2015).

6 Courtine, E., Selle, L. and Poinsot, T. DNS of intrinsic thermoacoustic modes in laminar premixed flames. *Combustion and Flame* **162**, 4331-4341, (2015).

7 Silva, C.F., Emmert, T., Jaensch, S. and Polifke, W. Numerical study on intrinsic thermoacoustic instability of a laminar premixed flame. *Combustion and Flame* **162**, 3370-3378, (2015).

8 Poinsot, T. and Veynante, D. *Theoretical and numerical combustion, 2nd edition*. Edwards, Philadelphia, (2005).

9 Truffin, K. Varoquie, B. and Poinsot, T. (2010). *Measurements of transfer functions using large eddy simulations: Theoretical framework and first tests*. [Online.] available: www.cerfacs.fr/~cfdbib/repository/TR_CFD_03_61.pdf

10 Vishnu, R. *Experimental study on combustion dynamics of a ducted lean premixed V-flame*. Master thesis, Indian Institute of Technology Madras, Department of Aerospace Engineering, (2013).